The Electron-Proton Bound State in the Continuum with the Positive Binding Energy of 1.531 of the Electron Mass

A. I. Agafonov[1,2]

[1]*National Research Centre "Kurchatov Institute", Moscow 123182, Russia*

[2]*Moscow Aviation Institute (National Research University), Moscow 125993, Russia*

Abstract

In the bound states in the continuum (BIC), the binding energy is positive, and the mass of a composite particle is greater than the total mass of its constituents. In this work, the BIC state is studied for the electron-proton system using the ladder Bethe-Salpeter equation. We demonstrate that there is a momentum space region in which the electromagnetic interaction between the particles is strongly enhanced, and the effective coupling constant is $\alpha\sqrt{m_p/m_e} = 0.313$, where α is the fine structure constant, and m_p and m_e are the proton and the electron masses. This interaction resonance causes the confinement of the pair in the BIC state with the positive binding energy of $1.531m_e$. The integral equation for the bispinor wave function is derived. This normalized wave function, which must be complex, was found numerically. It turned out that in the BIC state, the average radius for the electron is 48 Fm, and that for the proton is 1.1 Fm. This composite boson can exist exclusively in the free state, in which its properties, such as its form factors, should only be studied. In bound states with other particles, the composite loses its individuality. In Stern-Gerlach experiments, the electron-proton composite boson will demonstrate the properties of a spin $\frac{1}{2}$ fermion.

Keywords: composite particle, the bound states in the continuum, the electron-proton system, the interaction resonance

DOI: 10.31526/LHEP.2023.457

1. INTRODUCTION

Unlike the conventional bound states, there are the bound states in the continuum (BIC) in which the binding energy is positive and the composite particle mass is greater than the total mass of the constituents. The BIC states have been discovered by von Neumann and Wigner in 1929 [1] (see also [2] with some extension and correction of this work). The BIC states have been found experimentally in condensed matter physics and optics (see [3, 4, 5, 6, 7] and references therein). These states are stable due to the confinement mechanisms that are individual for each case.

In the nonrelativistic mechanics, the BIC states have been investigated by using the Schrödinger Hamiltonian. As a rule, the spectral analysis of the real equation $H\psi = E\psi$ with $E > 0$ was carried out [3, 4, 8, 9, 10]. However, this approach to BIC states is greatly simplified. The eigenvalues of the BIC states are in the continuous spectrum. Therefore, the study of the BIC states must be carried out using the Lippmann-Schwinger integral equation, in which an infinitesimal δ is added to the energy E. Then, the kernel of the integral equation and, respectively, the BIC wave functions become complex. As a result, the spectral analysis should be provided for a system of two coupled integral equations.

As far as we know in quantum electrodynamics the BIC states have not been supposed and studied previously. Furthermore, particle physics has been developed without the analysis of these states. Our idea is to apply this BIC phenomenon to some elementary particles. Below, we consider the system of the electron and the proton, and search for the BIC state of the system. This BIC state must represent a real particle.

The bound electron-proton system in the BIC state is a composite particle. Its charge is zero and spin is either 0 or 1. Therefore, this particle is the boson. Nevertheless, under certain experimental conditions, this boson with integer spin will manifest itself as a fermion with spin $\frac{1}{2}$. This unusual situation will occur, for example, in the Stern-Gerlach experiment, which is considered as a direct experiment to determine the spin of particles [11, 12]. Let a beam of particles split into two components in an inhomogeneous magnetic field. From this, one could conclude that these particles are fermions with spin $\frac{1}{2}$. However, this conclusion is erroneous, since the particles were the composite bosons. The observed splitting into two components is is due to the fact that the ratio of the spin-magnetic moment of the proton to the spin-magnetic moment of the electron is equal to $\frac{2.79}{\sqrt{3}}\frac{m_e}{m_p} = 0.877 \times 10^{-3}$.

Note that a beam of hydrogen atoms in the ground state would also split into two components, despite the fact that this atom is the boson. As is known, in such an experiment, the intrinsic magnetic moment of the electron was established [13].

In the BIC state, the boson mass m_B is greater than the sum of the electron and proton masses, $m_B > m_p + m_e$. The boson mass and wave function are the eigenvalue and eigenfunction of the kernel of an integral equation which will be obtained below.

It should be noted that the eigenvalue problem has, as a rule, analytical solutions only for the simplest one-particle differential or integral operators. Even for a two-electron atom, the problem is formulated as follows [14]. For a known energy level, it is required to find numerically the wave functions of the state. In another formulation, for given wave functions that have free parameters, it is necessary to find their values that result in the known energy values.

Of course, the integral equation for the BIC state is difficult to solve analytically. But this composite must represent a known particle. The only such particle is the neutron. In this case, the positive binding energy $\mathcal{E} = 1.531m_e$, and the energy eigenvalue of the composite is $m_B = m_p + m_e + \mathcal{E} =$

$m_p + 2.531m_e$. Then, the problem which is considered in the work is reduced to find the BIC wave functions of the particle.

The coupling constant of the electromagnetic interaction is the fine structure constant, $\alpha = \frac{1}{137.04}$. Because of the relatively small value of the coupling constant, the mass of the composite particle E in the normal bound states is slightly less than the mass of the constituent particles $\sum_i m_i$. Then, the binding energy defined as $E - \sum_i m_i$ is negative and, as a rule, is proportional to α^2. Typical examples are the hydrogen and the positronium.

In this regard, the following questions arise: (1) How can an electromagnetic interaction with the relatively small coupling constant lead to a composite particle with a large, positive value of the binding energy? (2) The composite from the electron and the proton is the boson with the spin equal to 0 or 1. Can the behavior of this boson in inhomogeneous magnetic fields represent fermion properties? The form factors of the composite boson can be extracted from the calculated wave function in the BIC state. Can these form factors be compared with the known data on the neutron form factors?

These issues are discussed in the present paper. The composite particle of the proton and the electron is studied. Using the ladder Bethe-Salpeter equation, an integral equation for the BIC state of the two-particle system is derived. We demonstrate that the electromagnetic interaction between the particles is strongly enhanced when the momenta of the constituents are in the two regions in the momentum space. These momentum-space regions can be called the resonant regions because the interaction between particles becomes formally unlimited. Together with the correlations in motion of the particles, the resonance of the electromagnetic interaction leads to the confinement of these particles in the BIC state with a positive binding energy equal to $1.531m_e$. A numerical solution of this integral equation by means of the iteration method is found. Results obtained for the BIC wave function in the momentum and coordinate spaces are presented.

Natural units ($\hbar = c = 1$) will be used throughout.

2. THE EQUAL-TIME BETHE-SALPETER EQUATION

Integral equations for a two-body system were derived by various methods (see Section 2 of the review [15]). Using the Feynman diagram technique, the general form of this equation was obtained by Bethe and Salpeter [16]. For scattering problems, of course, one should use the inhomogeneous Bethe-Salpeter equation. In order to study bound states, the homogeneous integral equation should be used for both negative and positive binding energies of the system [16]. In this case, bound states vanish as the coupling constant tends to zero.

The bound states are described by the homogeneous Bethe-Salpeter equation [16]:

$$\psi(1,2) = -i\int\int\int\int d\tau_3 d\tau_4 d\tau_5 d\tau_6 K_e(1,3) K_p(2,4) G(3,4;5,6)\psi(5,6). \tag{1}$$

In equation (1), $d\tau_i = d\mathbf{r}_i dt_i$, K_e and K_p are the free propagators for the electron and the proton, and $G(3,4;5,6)$ is the interaction function. In the ladder approximation, the function is given by

$$G^{(1)}(3,4;5,6) = -\alpha\left(1 - \boldsymbol{\alpha}_e\boldsymbol{\alpha}_p\right)\delta^{(4)}(3,5)\delta^{(4)}(4,6)\delta_+\left(s_{56}^2\right), \tag{2}$$

where $\delta_+(s_{56}^2)$ is the propagation function of the virtual photon.

Feynman discussed two different free-fermion propagators for the Dirac equation [17]:

$$K_+(2,1) = \sum_{\mathbf{p}} \psi_p(2)\bar{\psi}_p(1)\theta\left(t_2 - t_1\right) - \sum_{\mathbf{p}} \psi_{-p}(2)\bar{\psi}_{-p}(1)\theta\left(t_1 - t_2\right), \tag{3}$$

$$K_-(2,1) = \sum_{\mathbf{p}} \left(\psi_p(2)\bar{\psi}_p(1) + \psi_{-p}(2)\bar{\psi}_{-p}(1)\right)\theta\left(t_2 - t_1\right). \tag{4}$$

Here, $\psi_{\pm p}$ is the Dirac plane wave and $\bar{\psi}_p$ the Dirac conjugate wave function.

The modern description of the electron-positron field is based on the use of (3). The contribution to $K_+(2,1)$ for $t_2 > t_1$ is due to the electron terms, and the negative energy states are assumed to be not available to the electrons. The contribution to $K_+(2,1)$ for $t_2 < t_1$ is due to the positron terms, and the upper continuum is assumed to be not available to the positrons which are recognized as particles traveling backward in time [17]. As a result, the total number of degrees of freedom, which is determined by the complete basis of the Dirac plane waves, is divided into half. One-half of the degrees of freedom is assigned to the electron and the other to the positron.

Equation (4) determines the propagation of a free fermion which is described by the complete set of the Dirac plane waves.

As noted in [17], the choice of equation (4) is unsatisfactory to study relativistic field effects and (3) should be used. In contrast, the choice of equation (3) is unsatisfactory to study the motion of particles in external fields and (4) should be used [17].

There is no doubt that the complete spectrum of states for any system of interacting particles can be deduced only when the full basis of states is taken into account for each particle of the system [18]. In equation (4), the free-fermion states form the complete basis of the Dirac plane waves.

We study the BIC state for the electron which moves in the external field created by the proton. Then, equation (4) should be used. The free electron propagator (4) is reduced to the following form:

$$K_e(1,3) = \sum_{\mathbf{p}} \frac{1}{2\varepsilon_p}\left[\Lambda_e^+ e^{-i\varepsilon_p(t_1-t_3)} + \Lambda_e^- e^{i\varepsilon_p(t_1-t_3)}\right]\theta(t_1 - t_3)e^{i\mathbf{p}(\mathbf{r}_1-\mathbf{r}_3)}, \tag{5}$$

where

$$\Lambda_e^{\pm}(\mathbf{p}) = \varepsilon_{\mathbf{p}} \pm \boldsymbol{\alpha}_e\mathbf{p} \pm \beta_e m_e, \tag{6}$$

m_e, $\mathbf{p}$, and $\varepsilon_{\mathbf{p}} = \sqrt{m_e^2 + p^2}$ are the mass, the momentum, and the energy of the electron, and $\boldsymbol{\alpha}_e$ and β_e matrices are taken in the standard representation, $\beta_e = \left(\begin{smallmatrix} 1 & 0 \\ 0 & -1 \end{smallmatrix}\right)_e$, $\boldsymbol{\alpha}_e = \left(\begin{smallmatrix} 0 & \sigma_e \\ \sigma_e & 0 \end{smallmatrix}\right)$, and σ is the Pauli matrices. The subscript e of the Pauli matrices means their action on the spin of the particle e.

Respectively, the propagator of the particle p is given by

$$K_p(2,4) = \sum_{\mathbf{q}} \frac{1}{2\omega_q} \left[\Lambda_p^+ e^{-i\omega_q(t_2-t_4)} + \Lambda_p^- e^{i\omega_q(t_2-t_4)}\right] \theta(t_2-t_4)\, e^{i\mathbf{q}(\mathbf{r}_2-\mathbf{r}_4)}. \tag{7}$$

Here,

$$\Lambda_p^{\pm}(\mathbf{q}) = \omega_{\mathbf{q}} \pm \boldsymbol{\alpha}_p \mathbf{q} \pm \beta_p m_p, \tag{8}$$

m_p, $\mathbf{q}$, and $\omega_{\mathbf{q}} = \sqrt{m_p^2 + q^2}$ are the mass, the momentum, and the energy of the proton, and $\boldsymbol{\alpha}_p$ and β_p matrices are taken in the standard representation.

We search the BIC state with the binding energy proportional to the mass of the lighter particle from the pair, $\mathcal{E} \propto m_e$. The energy of the virtual photon, ω, is about the binding energy. We suppose that in the BIC state, the characterized scale of the distance between the two particles, r_{56}, is

$$r_{56} \ll \frac{m_e}{\mathcal{E}} \lambda\!\!\!^{-}_e, \tag{9}$$

where $\lambda\!\!\!^{-}_e$ is the Compton wavelength of the electron.

Obviously, (9) implies a physically reasonable size of the composite particle. Inequality (9) means that we can neglect the retardation of the interaction between the particles. Then, equation (1) is reduced to the equal-time Bethe-Salpeter equation:

$$\psi(\mathbf{r}_1, \mathbf{r}_2; E) = -\alpha \int d\mathbf{r}_1' \int d\mathbf{r}_2' \sum_{\mathbf{p}} \sum_{\mathbf{q}} K_{ep}(\mathbf{p}, \mathbf{q}; E) \times e^{i\mathbf{p}(\mathbf{r}_1-\mathbf{r}_1') + i\mathbf{q}(\mathbf{r}_2-\mathbf{r}_2')} \frac{1 - \boldsymbol{\alpha}_e \boldsymbol{\alpha}_p}{|\mathbf{r}_1' - \mathbf{r}_2'|} \psi(\mathbf{r}_1', \mathbf{r}_2'; E). \tag{10}$$

Here, the two-particle propagator is:

$$K_{ep} = \frac{1}{4\omega_q \varepsilon_p} \left[\frac{\Lambda_p^+ \Lambda_e^+}{E - \varepsilon_p - \omega_q + i\delta} + \frac{\Lambda_p^+ \Lambda_e^-}{E + \varepsilon_p - \omega_q + i\delta} + \frac{\Lambda_p^- \Lambda_e^+}{E - \varepsilon_p + \omega_q + i\delta} + \frac{\Lambda_p^- \Lambda_e^-}{E + \varepsilon_p + \omega_q + i\delta} \right]. \tag{11}$$

In the momentum space, equation (10) with (11) is reduced to the following form:

$$\psi(\mathbf{p}, \mathbf{q}; E) = -\frac{\alpha}{2\pi^2} K_{ep}(\mathbf{p}, \mathbf{q}; E) \int \frac{d\mathbf{k}}{k^2} \left(1 - \boldsymbol{\alpha}_e \boldsymbol{\alpha}_p\right) \psi(\mathbf{p} + \mathbf{k}; \mathbf{q} - \mathbf{k}). \tag{12}$$

3. RESONANCE OF THE ELECTROMAGNETIC INTERACTION

Consider the BIC state with the total energy $E = m_p + m_e + \mathcal{E}$ and the binding energy $\mathcal{E} = 1.531 m_e$. The imaginary parts of the last two terms in the square brackets in equation (13) vanish. These terms are not essential for the formation of the BIC state and can be omitted. The first two terms in equation (11) are fundamentally important. Using them, in equation (12), we can introduce a function describing the effective interaction between the particles:

$$\alpha_{\text{eff}} = \frac{\alpha \Lambda_e^+ \Lambda_p^+}{4\omega_q \varepsilon_p} \left[\frac{\mathcal{P}}{E - \varepsilon_p - \omega_q} - i\delta\left(E - \varepsilon_p - \omega_q\right) \right] + \frac{\alpha \Lambda_e^- \Lambda_p^+}{4\omega_q \varepsilon_p} \left[\frac{\mathcal{P}}{E + \varepsilon_p - \omega_q} - i\delta\left(E + \varepsilon_p - \omega_q\right) \right]. \tag{13}$$

For normal bound states, the energy eigenvalue is negative, $\mathcal{E} < 0$. Then, the δ-functions in the right-hand side of equation (13) vanish as well. Hence, any enhancement of the interaction between particles does not occur in the convenient bound states with the negative binding energy.

For the BIC state, the energy eigenvalue is positive, $\mathcal{E} > 0$. Hence, $E - m_p \pm m_e > 0$, and the term with the δ-function is principally important. This function determines the two regions in the momentum space which are solutions of the equation:

$$\left(E - \omega_{\mathbf{q}}\right)^2 = \varepsilon_{\mathbf{p}}^2. \tag{14}$$

Inside these regions, the principal part is

$$\frac{\mathcal{P}}{\left(E - \omega_q\right)^2 - \varepsilon_{\mathbf{p}}^2} = 0. \tag{15}$$

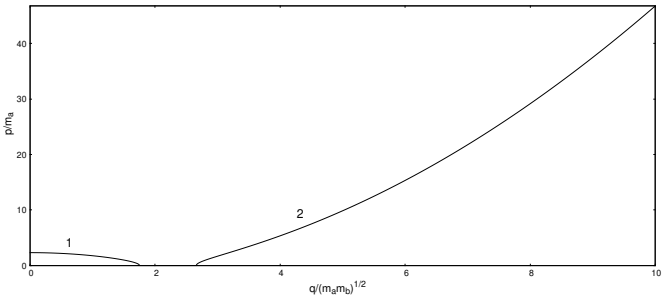

FIGURE 1: The solution of equation (14) for the energy $E = m_p + m_e + \mathcal{E}$ with $\mathcal{E} = \gamma m_e$ and $\gamma = 1.531$.

The two lines in Figure 1 correspond to the two regions in the momenta space. These lines are given the relation between the modules of the vectors $\mathbf{p}$ and $\mathbf{q}$. Their directions, $\mathbf{p}/p$ and $\mathbf{q}/q$, are also interrelated, as will be shown below. In these regions, the motions of two particles are correlated with each other, and their interaction is sharply enhanced, becoming formally unlimited. Therefore, these regions can be called resonant ones.

The first resonant region is presented by curve 1 in Figure 1. For the electron, this region is limited from above by the moment $p = 2.324 m_e$, and for the proton, the similar restriction is $q \leq 1.749\sqrt{m_e m_p}$. Here, the energies of both particles are positive. This curve is given by the first term in square brackets on the right side of equation (11). However, this region is not important for the formation of the BIC state that is of interest to us. This is because the electron momenta are relatively small. Respectively, it leads inevitably to a large radius of the composite particle that is about $\lambda\!\!\!^{-}_e$.

In this regard, the second resonant region represented by curve 2 in Figure 1 is of undoubted interest. It is determined by the second term in square brackets on the right side of equation (11). For this case, the proton energy, ω_q, is above the lower boundary ($+m_p$) of the upper continuum of the Dirac levels. At the same time, the electron energy, $-\varepsilon_p$, is negative, and is below the upper boundary ($-m_e$) of the lower continuum of the Dirac levels. In this region, the proton momentum $q \geq 2.659\sqrt{m_e m_p}$. We can estimate the characteristic radius of its motion in the BIC state: $R_{\text{eff}} < (2.659\sqrt{m_e m_p})^{-1}$. As for the $e-$ particle, there are no restrictions on its momentum. Moreover, the electron momentum increases sharply with q. It is important that this increase in the momenta p and q does not lead to a change in the energy $E = m_p + m_e + \mathcal{E}$.

Note that for normal bound states, finding a particle in lower continuum states is not uncommon. For example, in the bound states of the hydrogen, the electron is also characterized by a wave function in the lower continuum. But the probability of being in them is small, of the order of $\simeq \alpha^2$. This probability increases with the nuclear charge [19].

In the second resonant region, we have

$$\psi(\mathbf{p},\mathbf{q};E) = -\frac{\alpha}{8\pi^2\omega_q\varepsilon_p}\frac{\Lambda_e^-\Lambda_p^+}{E+\varepsilon_p-\omega_q+i\delta} \times \int_{D_k}\frac{d\mathbf{k}}{k^2}(1-\boldsymbol{\alpha}_e\boldsymbol{\alpha}_p)\psi(\mathbf{p}+\mathbf{k};\mathbf{q}-\mathbf{k}). \tag{16}$$

In equation (16), the integration over $\mathbf{k}$ is carried out in the second resonant region D_k:

$$m_p+(\gamma+1)m_e+\sqrt{m_e^2+(\mathbf{p}+\mathbf{k})^2}=\sqrt{m_p^2+(\mathbf{q}-\mathbf{k})^2}. \tag{17}$$

4. THE BIC WAVE FUNCTION IN THE MOMENTUM SPACE

From (17), we conclude that in the second resonant region the electron is relativistic and its momentum $p > m_e$. The proton is nonrelativistic. The proton energy can be written as $\omega_q = m_p + \frac{q^2}{2m_p}$, and its momentum $q \propto \sqrt{m_e m_p}$. Then, equation (8) is reduced to

$$\Lambda_p^+ \to 2m_p\begin{pmatrix}1&0\\0&0\end{pmatrix}_p. \tag{18}$$

Also, the interaction of the particles through the vector potential can be omitted since

$$\boldsymbol{\alpha}_e\boldsymbol{\alpha}_p \simeq \sqrt{\frac{m_e}{m_p}} \ll 1. \tag{19}$$

Due to the symmetry of the problem, the functions ψ can depend on absolute values of the vectors p and q and the angle between them θ. So, the function is $\psi(p,q;\theta)$. In the BIC state, the proton is non-relativistic and, taking into account (18), its spin part is the bispinor, in which only the upper spinor is nonzero, $\binom{a}{b}$ with constant a and b. This bispinor is not essential for further consideration.

In equation (16), the operator Λ_e^- given by (6) acts on the wave function $\psi(\mathbf{p}+\mathbf{k};\mathbf{q}-\mathbf{k})$. The spin operator and the orbital angular momentum operator each separately do not commute with the operator Λ_e^-. For this reason, the wave function cannot have a definite value of the orbital angular momentum and its z-projection [20]. Therefore, the function can be written as:

$$\psi(p,q;\theta)=\sqrt{\frac{\delta}{\pi}}\frac{1}{E+\varepsilon_p-\omega_q+i\delta}\begin{pmatrix}\frac{1}{\sqrt{3}}v(p,q;\theta)Y_{10}\left(\frac{\mathbf{p}}{p}\right)\\ \sqrt{\frac{2}{3}}v(p,q;\theta)Y_{11}\left(\frac{\mathbf{p}}{p}\right)\\ u(p,q;\theta)Y_{00}\\ 0\end{pmatrix}. \tag{20}$$

The bispinor (20) contains the spherical harmonics Y_{00}, Y_{10}, and Y_{11} with the azimuthal quantum number 0 and 1.

From (20), we obtain that the two-particle density is determined only in the second resonant region:

$$|\psi(p,q;\theta)|^2=\left(|v|^2+|u|^2\right)\delta\left(E+\varepsilon_p-\omega_q\right), \tag{21}$$

with the normalization condition:

$$\int d\mathbf{p}\int d\mathbf{q}\left(|v|^2+|u|^2\right)\delta\left(E+\varepsilon_p-\omega_q\right)=1. \tag{22}$$

Substituting (20) into (16) and considering (18)-(19), we obtain

$$\begin{pmatrix}v(\mathbf{p},\mathbf{q})\\u(\mathbf{p},\mathbf{q})\end{pmatrix}=\frac{i\alpha}{4\pi\varepsilon_p}\int_{D_k}\frac{d\mathbf{k}}{(\mathbf{k}-\mathbf{p})^2}\delta\left(E+\varepsilon_{\mathbf{k}}-\omega_{\mathbf{q}+\mathbf{p}-\mathbf{k}}\right) \times\begin{pmatrix}\left(\varepsilon_p-m_e\right)v\left(\mathbf{k};\mathbf{q}+\mathbf{p}-\mathbf{k}\right)-pu\\ \left(\varepsilon_p+m_e\right)u(\mathbf{k};\mathbf{q}+\mathbf{p}-\mathbf{k})-pv\end{pmatrix}, \tag{23}$$

where the second resonant region D_k is now defined as

$$m_p+(\gamma+1)m_e+\sqrt{m_e^2+k^2}=\sqrt{m_p^2+(\mathbf{q}+\mathbf{p}-\mathbf{k})^2}. \tag{24}$$

Note that in this region the principal part is

$$\frac{\mathcal{P}}{E+\varepsilon_{\mathbf{k}}-\omega_{\mathbf{q}+\mathbf{p}-\mathbf{k}}}=0. \tag{25}$$

5. TRANSFORMATION OF EQUATION (23)

Equation (23) is the integral equation with the imaginary kernel. So, the functions $v = v_r + iv_i$ and $u = u_r + iu_i$ must be complex. Then, in equation (23), there are four coupled integral equations for the four real functions $v_{r,i}(p,q,\theta)$ and $u_{r,i}(p,q,\theta)$. Without loss of generality, we can choose the vector $\mathbf{p}+\mathbf{q}$ that is directed along the z-axis. Then, equation (23) is rewritten as

$$\begin{aligned}&\begin{pmatrix}v_r(p,q,\theta)\\v_i(p,q,\theta)\\u_r(p,q,\theta)\\u_i(p,q,\theta)\end{pmatrix}\\ &=\frac{\alpha}{4\pi}\frac{m_p}{\varepsilon_p|\mathbf{q}+\mathbf{p}|}\int_0^\infty kdk\\ &\times\int_0^\pi\sin\theta_k\delta\left(\cos\theta_k-\frac{(\mathbf{q}+\mathbf{p})^2+k^2-q_*^2}{2k|\mathbf{q}+\mathbf{p}|}\right)\\ &\times\int_0^{2\pi}\frac{d\phi_k}{k^2+p^2-2kp\left(\cos\theta_k\cos\theta_p+\sin\theta_k\sin\theta_p\cos\phi_k\right)}\\ &\times\begin{pmatrix}-\left(\varepsilon_p-m_e\right)v_i\left(k,q_*,\theta_*\right)+pu_i\left(k,q_*,\theta_*\right)\\ \left(\varepsilon_p-m_e\right)v_r\left(k,q_*,\theta_*\right)-pu_r\left(k,q_*,\theta_*\right)\\ -\left(\varepsilon_p+m_e\right)u_i\left(k,q_*,\theta_*\right)+pv_i\left(k,q_*,\theta_*\right)\\ \left(\varepsilon_p+m_e\right)u_r\left(k,q_*,\theta_*\right)-pv_r\left(k,q_*,\theta_*\right)\end{pmatrix}.\end{aligned} \tag{26}$$

Here, using the property of the δ-function, $q_*(k) = |\mathbf{p}+\mathbf{q}-\mathbf{k}|$ is given by

$$q_*(k)=\sqrt{2m_p\left[(\gamma+1)m_e+\varepsilon_k\right]}, \tag{27}$$

with $\gamma = 1.531$, θ_* is the angle between the vectors $\mathbf{k}$ and $\mathbf{q}+\mathbf{p}-\mathbf{k}$,

$$\cos\theta_*=\frac{|\mathbf{q}+\mathbf{p}|\cos\theta_k-k}{q_*}, \tag{28}$$

ϕ_k and θ_k are the azimuthal and the polar angles of the vector $\mathbf{k}$,

$$\cos\theta_k=\frac{(\mathbf{q}+\mathbf{p})^2+k^2-q_*^2}{2k|\mathbf{p}+\mathbf{q}|}, \tag{29}$$

and θ_p is the polar angle of the vector $\mathbf{p}$; simple geometric considerations give us

$$\sin\theta_p = \frac{q\sin\theta}{|\mathbf{p}+\mathbf{q}|}. \tag{30}$$

After calculations of the integrals over the angles of the vector $\mathbf{k}$, equation (26) takes the following form:

$$\begin{aligned}
&\begin{pmatrix} v_r(p,q,\theta) \\ v_i(p,q,\theta) \\ u_r(p,q,\theta) \\ u_i(p,q,\theta) \end{pmatrix} \\
&= \alpha \frac{m_p}{2\sqrt{m_e^2+p^2}|\mathbf{q}+\mathbf{p}|} \\
&\times \int_{D_k} \frac{kdk}{\sqrt{\left(k^2+p^2-2kp\cos\theta_k\cos\theta_p\right)^2 - 4k^2p^2\sin^2\theta_k\sin^2\theta_p}} \\
&\times \begin{pmatrix} -\left(\varepsilon_p - m_e\right) v_i\left(k,q_*,\theta_*\right) + pu_i\left(k,q_*,\theta_*\right) \\ \left(\varepsilon_p - m_e\right) v_r\left(k,q_*,\theta_*\right) - pu_r\left(k,q_*,\theta_*\right) \\ -\left(\varepsilon_p + m_e\right) u_i\left(k,q_*,\theta_*\right) + pv_i\left(k,q_*,\theta_*\right) \\ \left(\varepsilon_p + m_e\right) u_r\left(k,q_*,\theta_*\right) - pv_r\left(k,q_*,\theta_*\right) \end{pmatrix}.
\end{aligned} \tag{31}$$

6. THE EFFECTIVE INTERACTION CONSTANT

Given $p \propto m_e$ and $k \propto m_e$, the integral on the right side of (31) is proportional to m_e. In the BIC state, the proton momentum $q \gg p$ and $q \propto \sqrt{m_p m_e}$. Taking into account the latter, the dimensionless factor before the integral in (29) is proportional to

$$\alpha_{\text{eff}} = \alpha\sqrt{\frac{m_p}{m_e}} = 0.313. \tag{32}$$

This value α_{eff} can be regarded as the effective interaction constant. The fact that $\alpha_{\text{eff}} \gg \alpha$ is caused by the resonance of the electromagnetic interaction between particles in the BIC state. Along with the angular correlations in the electron and proton motion, which are defined by the angle θ, this resonance effect determines the confinement mechanism of the composite particle in the BIC state [21].

7. THE COORDINATE-SPACE WAVE FUNCTION

The momentum-space wave function (20) satisfies the normalization (22). The coordinate-space wave function is defined as

$$\psi\left(\mathbf{r}_e,\mathbf{r}_p\right) = \frac{1}{(2\pi)^3}\int d\mathbf{q}\int d\mathbf{p}\psi(\mathbf{p};\mathbf{q})e^{-i\mathbf{p}\mathbf{r}_e - i\mathbf{q}\mathbf{r}_p}. \tag{33}$$

Here, $\mathbf{r}_e$ and $\mathbf{r}_p$ are the radius vectors of the electron and proton, respectively. Taking into account (31), the coordinate-space wave function is also normalized:

$$\int d\mathbf{r}_e\int d\mathbf{r}_p\left|\psi\left(\mathbf{r}_e,\mathbf{r}_p\right)\right|^2 = 1. \tag{34}$$

The function (33) can be presented in the following form:

$$\psi\left(\mathbf{r}_e,\mathbf{r}_p\right) = \begin{pmatrix} f\left(\mathbf{r}_e,\mathbf{r}_p\right) \\ g\left(\mathbf{r}_e,\mathbf{r}_p\right) \end{pmatrix}. \tag{35}$$

Here, f and g are complex functions which are given by the following equation:

$$\begin{aligned}
&\begin{pmatrix} f\left(\mathbf{r}_e,\mathbf{r}_p\right) \\ g\left(\mathbf{r}_e,\mathbf{r}_p\right) \end{pmatrix} \\
&= N\int d\mathbf{q}\int d\mathbf{p}\delta\left(q^2 - q_*^2(p)\right)\begin{pmatrix} v\left(\mathbf{p},\mathbf{q}\right)\cos\theta_p \\ u\left(\mathbf{p},\mathbf{q}\right) \end{pmatrix} e^{-i\mathbf{p}\mathbf{r}_e - i\mathbf{q}\mathbf{r}_p},
\end{aligned} \tag{36}$$

where N is the normalization factor.

8. DETAILS OF CALCULATIONS

It is convenient to use the dimensionless quantities: $x = p/m_e$, $y = q/\sqrt{m_e m_p}$, $z = k/m_e$. Then, using the notation $\eta = \sqrt{\frac{m_e}{m_p}}$, equation (31) takes the following form:

$$\begin{aligned}
&\begin{pmatrix} v_r(x,y,\theta) \\ v_i(x,y,\theta) \\ u_r(x,y,\theta) \\ u_i(x,y,\theta) \end{pmatrix} \\
&= \frac{\alpha_{\text{eff}}}{2\sqrt{1+x^2}\sqrt{y^2+2\eta xy\cos\theta+\eta^2x^2}} \\
&\times \int_{D_z} \frac{zdz}{\sqrt{\left(z^2+x^2-2xz\cos\theta_z\cos\theta_x\right)^2 - 4z^2x^2\sin^2\theta_z\sin^2\theta_x}} \\
&\times \begin{pmatrix} -\left(\sqrt{1+x^2}-1\right) v_i\left(z,t_*,\theta_*\right) + xu_i\left(z,t_*,\theta_*\right) \\ \left(\sqrt{1+x^2}-1\right) v_r\left(z,t_*,\theta_*\right) - xu_r\left(z,t_*,\theta_*\right) \\ -\left(\sqrt{1+x^2}+1\right) u_i\left(z,t_*,\theta_*\right) + xv_i\left(z,t_*,\theta_*\right) \\ \left(\sqrt{1+x^2}+1\right) u_r\left(z,t_*,\theta_*\right) - xv_r\left(k,t_*,\theta_*\right) \end{pmatrix}.
\end{aligned} \tag{37}$$

The notations (27)–(30) are rewritten as

$$t_*(z) = \sqrt{2\left(\gamma+1+\sqrt{1+z^2}\right)}, \tag{38}$$

$$\cos\theta_*(x,y,\theta,z) = \frac{1}{t_*}\left[\sqrt{y^2+2\eta xy\cos\theta+\eta^2x^2}\cos\theta_z - \eta z\right], \tag{39}$$

$$\cos\theta_z(x,y,\theta,z) = \frac{y^2+2\eta xy\cos\theta+\eta\left(x^2+z^2\right)-t_*(z)^2}{2\eta z\sqrt{y^2+2\eta xy\cos\theta+\eta^2x^2}}, \tag{40}$$

$$\sin\theta_x = \frac{y\sin\theta}{\sqrt{y^2+2\eta xy\cos\theta+\eta^2x^2}}. \tag{41}$$

From (22), we obtain the normalization condition:

$$\begin{aligned}
8\pi^2\int_0^\infty x^2t_*(x)dx\int_0^\pi\sin\theta d\theta\Big[&\left|v\left(x,t_*(x),\theta\right)\right|^2 \\
&+\left|u\left(x,t_*(x),\theta\right)\right|^2\Big] = 1.
\end{aligned} \tag{42}$$

For the coordinate-space wave function, we introduce the dimensionless variables, $s = m_e r_e$, $t = \sqrt{m_e m_p}r_p$ and the angle θ_r between $\mathbf{r}_e$ and $\mathbf{r}_p$. Assuming that, without loss of generality,

$\mathbf{r}_p$ is directed along the z-axis, equation (36) is rewritten as

$$\begin{aligned}
&\begin{pmatrix} f(s,t,\theta_r) \\ g(s,t,\theta_r) \end{pmatrix} \\
&= N \int_0^\infty x^2 t_*(x) dx \\
&\quad \times \int_0^\pi J_0\left(sx \sin\theta_r \sin\theta_p\right) e^{-isx\cos\theta_p \cos\theta_r} \sin\theta_p d\theta_p \\
&\quad \times \int_0^\pi e^{-it*t_*(x)\cos\theta_q} \sin\theta_q d\theta_q \int_0^{2\pi} \begin{pmatrix} v(x,t_*(x),\theta)\cos\theta_p \\ u(x,t_*(x),\theta) \end{pmatrix} d\phi_q.
\end{aligned} \tag{43}$$

Here, the normalization factor N is determined by the normalization condition, which is easily found in (33), J_0 is the Bessel function of the first kind, and

$$\cos\theta = \cos\theta_p \cos\theta_q + \sin\theta_p \sin\theta_q \cos\phi_q. \tag{44}$$

All the numerical values, which are given throughout the paper, were obtained using the electron and proton masses and the positive value of binding energy $\mathcal{E} = 1.531 m_e$. The reason for this binding energy is discussed in Section 1. There are no free or fitting parameters in the presented theory.

9. NUMERICAL RESULTS

9.1. Momentum-Space BIC Wave Function

According to equation (37), the momentum-space wave function $\psi(p,q;\theta)$ is determined by the four real functions v_r, v_i, u_r, and u_i. They depend on three variables p, q, and θ and are interrelated with each other. For the positive binding energy $1.531 m_e$, the solution of this equation was found numerically using the iteration method. The functions $v_{r,i}(p,q,\theta)$ and $u_{r,i}(p,q,\theta)$ were represented with matrices of the dimension $201 \times 201 \times 101$.

It was obtained that for any given angle θ, all these functions represent the single peak located in the same place on the (p,q) plane. The height of the peak changes with the angle. Moreover, it is a sign of alternating. The heights of peaks are significantly different from zero only for a certain interval of the angles θ.

The value $q_*(p) = \sqrt{2m_p[(\gamma+1)m_e + \varepsilon_p]}$ with $\gamma = 1.531$ can be considered as the characteristic momentum of the proton in the bound state. The point (p, q_*) does not correspond to the maximum of the peaks but falls within the location of the peaks on the (p,q) plane. In Figures 2 and 3, we show these four functions depending on the electron momentum p and the angle θ for the given proton momentum $q_*(p)$. It can be seen that the main peaks cluster around the angles $\theta \simeq [\pi/18, \pi/4]$. Outside this angular region, these four functions are very small. Data shown in Figures 2 and 3 represent the momentum-space BIC wave function of the electron-proton system.

This BIC state of the bound electron-proton system is not the ground state, which is nondegenerate for any quantum system. Excited states are, as a rule, degenerate. Therefore, equation (37) can have several solutions for the given binding energy.

In addition to the state shown in Figures 2 and 3, one more solution of equation (37) has been obtained. For this second solution, the functions v_r, v_i, u_r, and u_i also represent the single peak with variable height depending on the angle θ.

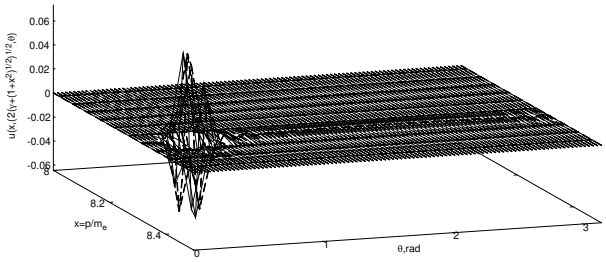

FIGURE 2: The functions $u_r(p, q_*(p), \theta)$ (solid line) and $u_i(p, q_*(p), \theta)$ (dashed line).

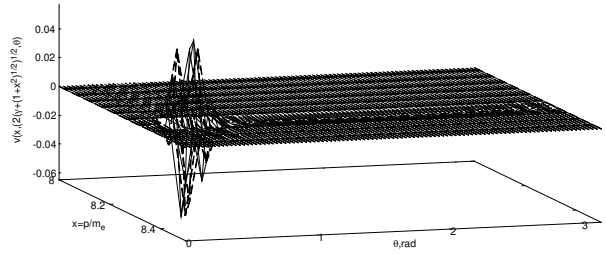

FIGURE 3: The functions $v_r(p, q_*(p), \theta)$ (solid line) and $v_i(p, q_*(p), \theta)$ (dashed line).

The results for this second solution are demonstrated in Figures 4 and 5. They are close to those presented in Figures 2 and 3. However, the angular positions of the peaks are shifted relative to those for the first solution. The shift angle is approximately equal to $\pi/2$.

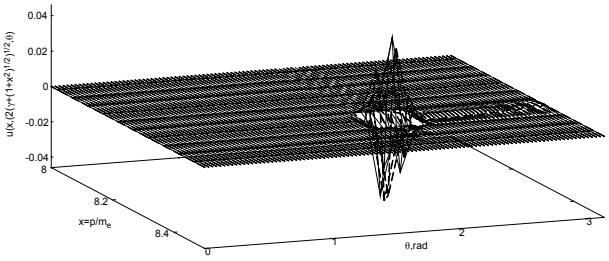

FIGURE 4: The functions $u_r(p, q_*(p), \theta)$ (solid line) and $u_i(p, q_*(p), \theta)$ (dashed line) for the second solution of equation (37).

The two momentum-space BIC wave functions, discussed above, are the eigenfunctions of the integral equation (37) with the eigenvalue $E = m_p + 2.531 m_e$.

9.2. Coordinate-Space BIC Wave Function

The coordinate-space BIC wave function $\psi(r_e, r_p, \theta_r)$ was calculated from (43). Since the momentum-space wave functions are normalized, the coordinate-space wave function must also satisfy the normalization condition (34). For the numerical solution of equation (43), the function $\psi(\mathbf{r}_e, \mathbf{r}_p)$ was replaced by the matrix with the dimension $121 \times 121 \times 17$. Such small dimen-

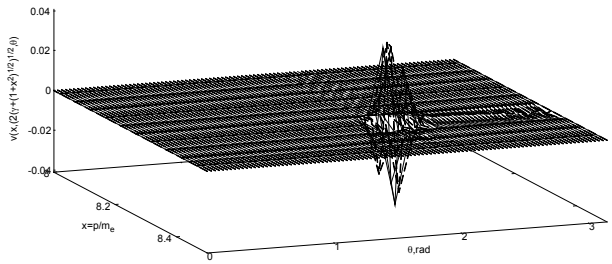

FIGURE 5: The functions $v_r(p, q_*(p), \theta)$ (solid line) and $v_i(p, q_*(p), \theta)$ (dashed line) for the second solution of equation (37).

sion is due to the many nested loops involved in the numerical procedure. Of course, this small dimension could affect the accuracy of the calculations. However, the use of matrices with the dimension of $101 \times 101 \times 17$ does not lead to a significant change in the calculation results.

Note that we did not find a significant difference in the coordinate-space wave functions which have been calculated for these two momentum-space wave functions discussed above.

As it follows from (18), in the BIC state, the proton is only in the states of the upper continuum. The state of the electron is determined by the bispinor (35), which contains two complex functions f and g. These functions f and g determine the probabilities of finding the electron in the states of the upper and lower continua, respectively. It turned out that the function f is very small compared to the function g.

For the sake of completeness, the real part of the function f is shown in Figure 6 for the angle $\theta_r = \pi/2$. For this angle, the function f is close to maximal. Noteworthy are the very small values of this function. These values are so small that cannot affect the normalization of ψ.

Thus, the probability of finding the electron in the states of the upper continuum is negligible. The electron with a probability close to one is in the states of the lower continuum.

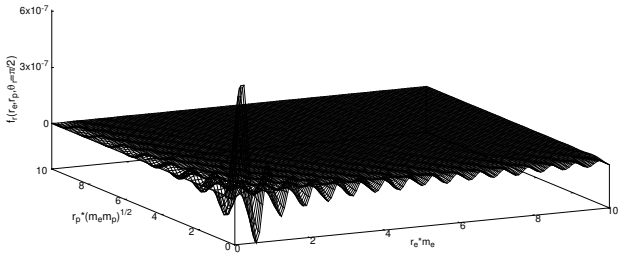

FIGURE 6: The functions $f_r(r_e, r_p, \theta_r = \pi/2)$.

Now, the complex function $g = g_r + ig_i$ is analyzed. It depends on the angle θ_r between the electron ($\mathbf{r}_e$) and the proton ($\mathbf{r}_p$) radius-vectors. According to the calculations, these two functions g_r and g_i have similar dependencies on r_e and r_p for a given angle θ_r. However, the real part g_r has, as a rule, large values compared to g_i.

The function g_r is relatively small at small angles $\theta_r \simeq 0$ and for the angles near π. This function is shown in Figure 7 for the angle $\theta_r = 0$. Attention is drawn to the peak $g_r(0, 0)$. This peak will be present at all other angles. According to Figure 7, with the highest probability density, the electron and the proton are near the positions $r_e = 0$ and $r_p = 0$.

The values of the g function increase with the angle. As shown in Figure 8, for $\theta_r = \pi/4$, the function $g_r(r_e, r_p, \theta_r = \pi/4)$ has also a narrow peak near $r_e \simeq 0$ and $r_p \simeq 0$. Outside this peak, this function has significantly smaller values. As r_e and r_p increase, the behavior of g_r corresponds to damped oscillations around zero.

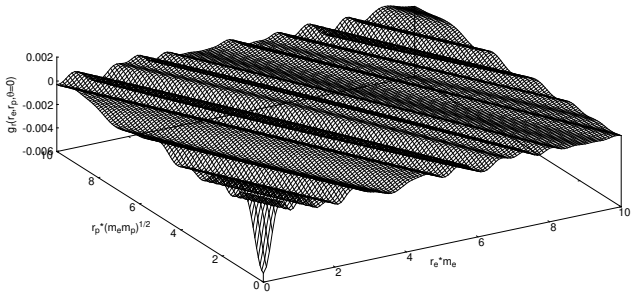

FIGURE 7: The functions $g_r(r_e, r_p, \theta_r = 0)$.

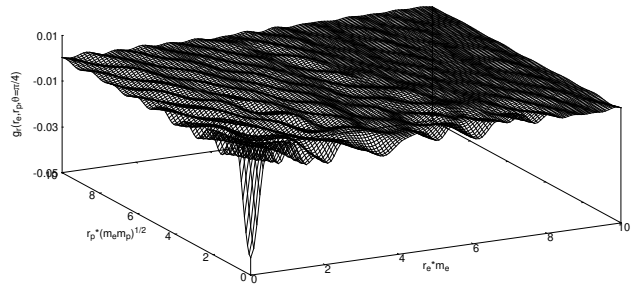

FIGURE 8: The functions $g_r(r_e, r_p, \theta_r = \pi/4)$.

The structure of the function g is the same up to the angle $\pi/2$. So, the differences between the functions at $\theta_r = \pi/4$ and $\theta_r = \pi/2$ are quite insignificant. Further, as the angle increases, the situation changes. The central peak is preserved. However, outside the peak, the oscillatory behavior of the g function becomes stronger. This behavior for the angle $3\pi/4$ is demonstrated in Figure 9.

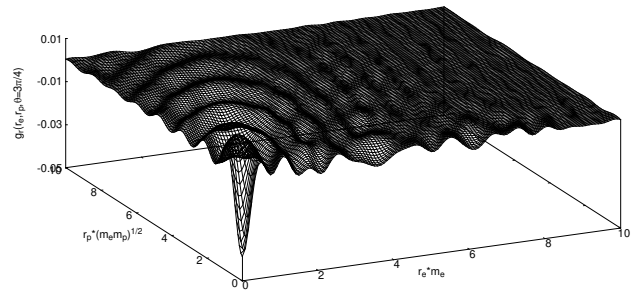

FIGURE 9: The functions $g_r(r_e, r_p, \theta_r = 3\pi/4)$.

The function decreases as the angle θ_r approaches π. Figure 10 shows the function g_r for $\theta_r = \pi$. The characteristic values of

the function are an order of magnitude smaller than those for the angle $\theta_r = 3\pi/4$. The central peak has been transformed into a deep dip on the undulating surface $g_r(r_e, r_p)$.

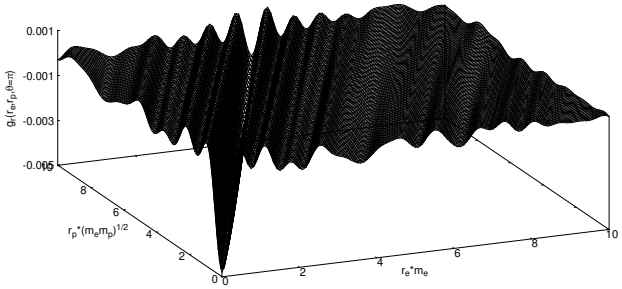

FIGURE 10: The functions $g_r(r_e, r_p, \theta_r = \pi)$.

The electron-proton BIC state with the positive binding energy can be characterized by the average values of the electron radius $\langle r_e \rangle$ and the proton radius $\langle r_p \rangle$. These averages were calculated as follows:

$$\begin{pmatrix} \langle r_e \rangle \\ \langle r_p \rangle \end{pmatrix} = \int d\mathbf{r}_e \int d\mathbf{r}_p \begin{pmatrix} r_e \\ r_p \end{pmatrix} |\psi(\mathbf{r}_e, \mathbf{r}_p)|^2 . \quad (45)$$

The integration in equation (45) is carried out over the plan $r_e \leq 10/m_e$ and $r_p \leq 10/\sqrt{m_e m_p}$. According to the obtained data for the wave function, which are partially presented in Figures 6–10, the values of $\langle r_e \rangle m_e$ and $\langle r_p \rangle \sqrt{m_e m_p}$ are very close. We obtained $\langle r_e \rangle = 0.124/m_e = 48\,\text{Fm}$ and $\langle r_p \rangle = 0.120/\sqrt{m_e m_p} = 1.1\,\text{Fm}$.

10. CONCLUSION

In the present work, the theory of BIC states of composite particles was supplemented with the conception of the resonance of interaction between the constituent particles. Using the two particle Bethe-Salpeter equation, the resonant regions in momentum space are found with the sharp increase in the electromagnetic interaction between the electron and the proton. This increase is so strong that the effective coupling constant is equal to $\alpha\sqrt{m_p/m_e} = 0.313$. Along with correlations in the electron and proton motion, this resonance effect determines the confinement mechanism of the composite particle in the BIC state with the positive binding energy of 1.531 of the electron mass. It was obtained that, in the BIC state, the average radius for the electron is equal to 48 Fm, and the average radius for the proton is equal to 1.1 Fm.

This BIC state must represent a real particle. In the BIC state which is found, the boson mass m_B is greater than the sum of the electron and proton masses, $m_B = m_p + 2.531m_e$. The charge of the boson is zero, and its spin is an integer, but the boson will demonstrate the one-half spin in the Stern-Gerlach-like experiments. This is due to the fact that the nuclear magneton is very small compared to the Bohr magneton. That is, this composite particle could be the *free* neutron. Here, the word "free" is very important.

Experimental data on the charge and magnetic form factors of the neutron would allow us to determine the structure of the neutron. Of course, one means the structure of the free neutron. However, to my knowledge, there are no direct measurements of free-neutron form factors. As a rule, electron scattering cross-section measurements on the deuteron (d) and helium-3 (^3_2He) targets are intensively carried out [22, 23, 24]. Then, using proton form factors and the fitting procedure [25], the neutron form factors have been extracted from this scattering data. In these experiments, the properties of the free neutron are not studied.

The neutron is a composite particle both in the quark model and in the BIC electron-proton model that we are considering. All fundamental properties of the neutron are determined only for the free neutron [26]. The free particle is characterized by the wave function that determines the properties of the composite, such as its mass, charge, and spin form factors. When the composite particle interacts with other particles, or when it combines with other composites, its structure changes, the free-state wave function vanishes, and the properties of the free composite are lost. Therefore, composite particles exist only in the free state. That is, the compound neutron in the free state and what it was transformed, for example, in the helium nucleus or the carbon nucleus are different objects.

Using the wave function obtained in the BIC model of the neutron, we can calculate, for example, its charge form factor. However, there is nothing to compare it with, since we did not find any experimental works on measuring the form factors of free neutrons in the literature. Despite all the complexity, the physical properties of such particles should be studied only when they are free.

CONFLICTS OF INTEREST

The author declares that there are no conflicts of interest regarding the publication of this paper.

ACKNOWLEDGMENTS

The work was carried out within the state assignment of National Research Centre "Kurchatov Institute."

References

[1] J. von Neumann and E. Wigner, Über merkwürdige diskrete Eigenwerte, Phys. Z. 1929, 30, 465.
[2] F. H. Stillinger and D. R. Herrick, Bound states in the continuum, Phys. Rev. A 1975, 11, 446.
[3] C. W. Hsu, B. Zhen, A. D. Stone, J. D. Joannopoulos, and M. Soljačić, Bound states in the continuum, Nat. Rev. Mater. 2016, 1, 16048.
[4] A. F. Sadreev, Interference traps waves in open system: Bound states in the continuum, Reports on Progress in Physics 2021, 84, 055901.
[5] M. Robnik, A simple separable Hamiltonian having bound states in the continuum. J. Phys. A: Math. Gen. 1986, 19, 3845.
[6] F. Capasso, C. Sirtori, J. Faist, D. L. Sivco, S.-N. G. Chu, and A. Y. Cho, Observation of an electronic bound state above a potential well. Nature 1992, 358, 565.
[7] S. I. Azzam and A. V. Kildishev, Photonic bound states in the continuum: from basics to applications, Adv. Opt. Mater. 2021, 9, 2001469.

[8] F. Odeh, Note on differential operators with purely continuous spectrum, Proc. Amer. Math. Soc. 1965, 16, 363.
[9] T. Kato, Some Mathematical Problems in Quantum Mechanics, Prog. Theor. Phys. Suppl. 1967, 40, 3.
[10] B. Simon, On positive eigenvalues of one-body Schrödinger operators, Commun. Pure Appl. Math. 1969, 22, 531–538.
[11] J. E. Sherwood, T. E. Stephensen, and S. Bernstein, Stern-Gerlach Experiment on Polarized Neutrons, Phys. Rev. 1954, 96, 1546.
[12] D. J. Hughes and M. T. Burgy, Reflection of Neutrons from Magnetized Mirrors, Phys. Rev. 1951, 81, 498.
[13] T. E. Phipps, The Magnetic Moment of the Hydrogen Atom, Phys. Rev. 1927, 29, 309.
[14] H. A. Bethe and E.E. Salpeter, Quantum Mechanics of One- and Two-Electron Atoms, Springer, Berlin, 1957.
[15] N. Nakanishi, A General survey of the theory of the Bethe-Salpeter equation, Prog. Theor. Phys. Suppl. 1969, 43, 1.
[16] H. A. Bethe and E. E. Salpeter, A Relativistic Equation for Bound-State Problems, Phys. Rev. A 1951, 84, 1232.
[17] R. P. Feynman, The Theory of Positrons, Phys. Rev. 1949, 76, 749.
[18] A. I. Agafonov, Massless Composite Bosons Formed by the Coupled Electron-Positron Pairs and Two-Photon Angular Correlations in the Colliding Beam Reaction $e^-e^+ \rightarrow B\gamma\gamma$ with Emission of the Massless Boson, Advances in High Energy Physics, vol. 2018, Article ID 6137380, 18 pages, 2018.
[19] Ya. B. Zel'dovich and V. S. Popov, Electronic structure of superheavy atoms, Sov. Phys. Usp. 1972, 14, 673.
[20] V. B. Berestesky, E. M. Lifshits, and L. P. Pitaevsky, Quantum electrodynamics, Fizmatlit, Moscow, 2002.
[21] A. I. Agafonov, Resonance enhancement of the electromagnetic interaction between two charged particles in the bound state in the continuum, Mod. Phys. Lett. A, 2023, 38, 2350070.
[22] V. Punjabi, C. F. Perdrisat, M. K. Jones, E. J. Brash, and C. E. Carlson, The Structure of the Nucleon: Elastic Electromagnetic Form Factors, Eur. Phys. J., 2015, A 51, 79.
[23] G. Warren, F. Wesselmann, H. Zhu et al. (Jefferson Lab E93-026 Collaboration), Measurement of the Electric Form Factor of the Neutron at $Q^2 = 0.5$ and $1.0\,\mathrm{GeV}^2/\mathrm{c}^2$, Phys. Rev. Lett. 2004, 92, 042301.
[24] B. S. Schlimme et al. (A1 collaboration), Measurement of the Neutron Electric to Magnetic Form Factor Ratio at $Q^2 = 1.58\,\mathrm{GeV}^2$ using the Reaction ${}^3\vec{H}e(\vec{e},e',n)pp$, Phys. Rev. Lett. 2013, 111, 132504.
[25] Zh. Ye, J. Arrington, R. J. Hill, and G. Lee, Proton and neutron electromagnetic form factors and uncertainties, Physics Letters B, 2018, 777, 8.
[26] A. I. Frank, Fundamental properties of the neutron: Fifty years of research, Sov. Phys. Usp., 1982, 25, 280–297.